ON DESIGN OF AN ADAPTIVE PSO-FUZZY LOGIC-BASED SPEED CONTROL SCHEME FOR SWITCHED RELUCTANCE MOTOR DRIVES

ThiMaiPhuong DAO[1,2] Yaonan WANG[1]
[1]College of Electrical and Information Engineering
Changsha, Hunan 410082, China, Phone: +86 13088051248, Email: daophuong@haui.edu.vn
[2]Faculty of Electrical Engineering Technology, Hanoi University of Industry, Hanoi, Vietnam

NgocKhoat NGUYEN[3,4]
[3]School of Energy Science and Engineering, University of Electronic Science and Technology of China
[4]Faculty of Automation Technology, Electric Power University, Hanoi, Vietnam
Phone: +84 916141764, Email: khoatnn@epu.edu.vn

Abstract: *In this paper, Particle Swarm Optimization (PSO) method, which is one of the most effective biological-inspired optimization algorithms, will be applied to design an adaptive Fuzzy Logic (FL)-based speed control strategy for Switched Reluctance Motor (SRM) drives. The PSO mechanism is used to not only optimize three scaling factors of a PI-type FL speed controller but also determine efficiently two switching angles of an asymmetrical DC-DC voltage converter which would be highly consistent with the SRM feeding. The control methodology applying each of the five-optimal-parameter groups obtained is capable of achieving effective control performances for a particular SRM drive system, such as short rise time, non-overshoot and highly small reduction of the speed despite the occurrence of load torques. In addition, the starting and running torques are of high values to be suitable for designing an effective traction control system. It is found that these promising features are much better than those of the conventional PI-based scheme applied to the SRM drive system. To achieve the obvious validation with respect to the efficiency, feasibility and superiority of the proposed control strategy, numerical simulations for a typical three phase SRM drive with various cases of the load torques will also be performed using MATLAB/Simulink package.*

Key words: *Switched Reluctance Motor, Particle Swarm Optimization, PI, PI-type FL controller, Switching Angles.*

1. Introduction

Due to some of significant advantages including low cost, simple-rugged construction, reliable operation and wide speed control range, Switched Reluctance Motors (SRMs) have been applied efficiently in plenty of practical drive systems requiring the variable speed [1-5]. The applications of these SRM drive systems are to focus on (i) designing the traction drive control systems of Electric Vehicles (EVs) [6, 7], hybrid EVs [8], and Plug-in hybrid EVs [9]; (ii) particular function systems, e.g., generators of renewable energy systems [10] and (iii) industrial drive systems: machining machineries, washing machines, mining drives, etc. [4] Together with the typical prototypes, such as 6/4 (three phases) and 8/6 (four phases), the novel kinds of the SRMs have been continuously investigating in order to seek the perfect structures of electrical machines for the future of effective drive systems [11-13].

The SRMs, in spite of their increasing applications, are still being studied to deal with their inherent disadvantages, e.g., the nonlinearity, the torque ripple and the difficult control of electronic power converters, which are used to feed the energy to the machines [14-16]. It is found that the efficient control strategies need to be investigated to obtain the permissible control performances, such as the stability, high efficiency and the optimal dynamic responses of the phase current, electromagnetic torque as well as the angular speed. In general, control strategies, which mainly focus on designing speed and current controllers, have applied both the conventional and modern regulators. The conventional controllers (i.e., PI and PID regulators) have been considered initially due to their simplicity of the design and operation [3,17]. Nevertheless, the poor control characteristics obtained, such as the high overshoot, the long rise and settling time as well as the large reduction of speed due to load torque, have restricted the widespread use of such controllers, particularly in the drive systems requiring high quality, e.g., the traction drives of EVs. Hence, these regulators should be replaced with the improved controllers using the modern techniques, e.g., Fuzzy Logic (FL), in order to attain the better control properties. Based on the FL technique, the PI-type FL controllers (FLCs) have been applied widely and efficiently in many control systems [18-20], especially in the SRM drives.

Applying such a PI-type FLC for a speed regulator and/or a current controller, the scaling factors, which affect significantly the control performances of the drive system, must be tuned properly in order to obtain the desired quality and efficiency. Many reports have been published to deal with this problem [19-21]. However, the SRM drive system, which is supplied by an electronic power converter (e.g., an asymmetrical DC-DC inverter), is usually subjected to the switching

states of the semiconductor devices [3]. This leads to the difficulty of the control strategies to achieve entirely the permissible characteristics. Basically, an optimal control strategy applying the FLCs has to make sure that not only the parameters of such FLCs but also the switching angles of the inverter should be optimized successfully.

In order to conduct the above problem, Particle Swarm Optimization (PSO) method, which is one of the most effective biological-inspired optimization techniques [22-24], will be applied in this study. With an online implementation through several appropriate steps, the PSO mechanism is able to optimize effectively three scaling factors of the PI-type FLC (two inputs and one output) as well as two switching angles (turn-ON and turn-OFF angles) of the voltage-source DC-DC converter. Resulting from such an optimization process, five parameters obtained can be used to design an adaptive control strategy based on the PI-type FL architecture for a particular SRM drive. In this paper, a three-phase SRM model (6/4-type machine) is selected for the simulation aim to validate the feasibility of the proposed control scheme. Based on the PSO algorithm, two simulation cases, including for tuning only the scaling factors of the FL architecture and for all the FLC and switching angles, with various cases of load torques will be performed. Applying both the PSO-PI-type FLC and the conventional PI regulator to design the speed controllers, simulation results obtained are able to be used to verify the effectiveness and superiority of the proposed control methodology.

The rest of this paper is organized as follows. Section 2 presents a method to mathematically model an SRM, which will be applied to justify the effectiveness of the control strategies. Section 3 then describes a fundamental architecture of a PI-type FL speed controller used for the SRM drive. The design of the adaptive PI-type FL speed control methodology based on the PSO algorithm will be mentioned specifically in Section 4. Subsequently, the feasibility and effectiveness of the proposed strategy validated through numerical simulation processes will be presented in Section 5. Finally, conclusion, discussion and future work are also described in Section 6.

2. Mathematical Model of the SRM Drive

With respect to the physical structure, an SRM should be considered as a doubly salient pole and singly excited machine. The SRM is typically fed by a DC power source, such as a voltage- or current-type DC source feeding. Thus, a unipolar electric power inverter, e.g., DC-DC or AC-DC converter, can be used. Figure 1(a) shows the cross-section of a typical family of the SRMs, i.e., 8/6-type SRM. Here, the stator has 8 poles (4 pole-pairs wound by serially concentrated windings) corresponding to 4 phases: A, B, C and D. Meanwhile, the rotor, which is composed of neither windings nor magnets, has 6 poles (see Figure 1(a)). The configuration of the k-th phase winding connected to the corresponding phase of an asymmetrical DC-DC inverter is described in Figure 1(b). Despite the simplicity of the construction, it is highly difficult to design an exact mathematical model of an SRM due to its nonlinear characteristics. All of its characteristics including flux linkage, inductance and torque are nonlinearly dependent upon the variation of not only the phase current but also the rotor position during the operation of the machine [2-4]. In order to simplify the modeling process, each phase of the SRM can be replaced with an equivalent circuit, including a winding resistance in series with an inductance as shown in Figure 1(c). Such inductance will be considered as a function of both the phase current and the rotor position when computing the flux linkage of the k-th phase as expressed below:

$$\Psi_k(i_k,\theta)=\sum_{l=1}^{n}L_{kl}(i_k,\theta).i_k(t) \qquad k=1,2,...\text{n} \quad (1)$$

where $\Psi_k(i_k,\theta)$, $i_k(t)$ and θ denote the flux linkage, phase current and rotor position of the k-th phase, respectively. Meanwhile, the value of $L_{kl}(i_k,\theta)$, which is a mutual inductance between the k-th phase and the l-th phase, can be neglected since it would be much smaller than the corresponding bulk inductance in practice [3-4].

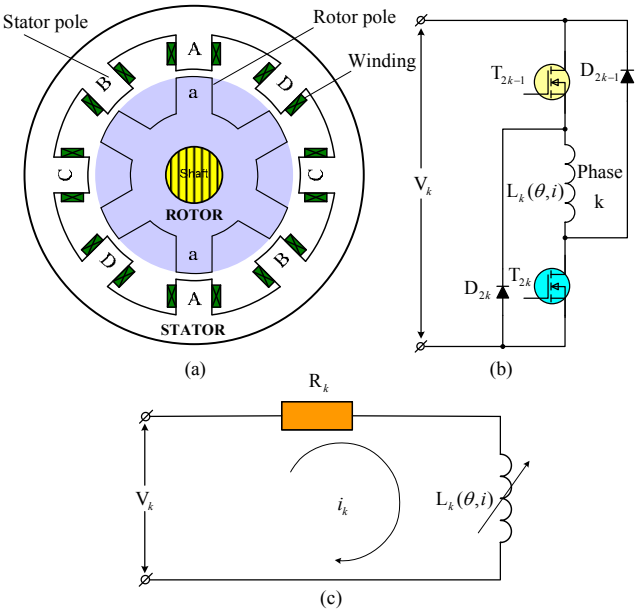

Figure 1: A typical configuration of 8/6-type SRM
(a) Cross-section
(b) Phase k-th feeding
(c) An equivalent circuit for the k-th phase

Theoretically, the instantaneous k-th phase voltage of the SRM $V_k(t)$ can be calculated as:

$$V_k(t)=R_k i_k(t)+\frac{d\Psi_k(i_k,\theta)}{dt} \quad (2)$$

where R_k is the winding resistance of the k-th phase. From (1) and (2), using the derivative calculus of multivariable functions, one can be obtained below:

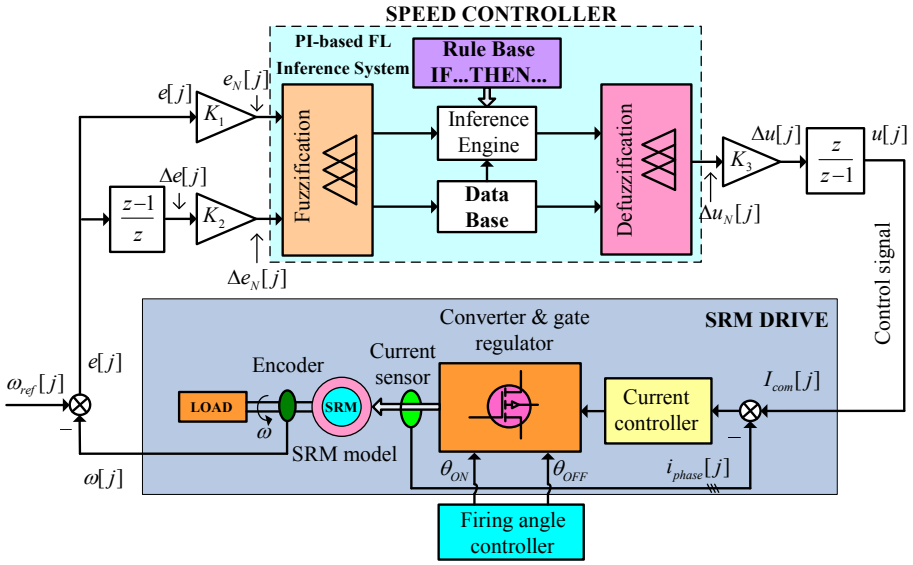

Figure 2: The fundamental architecture of a PI-type FL speed controller for SRM

$$V_k(t) = R_k i_k(t) + \sum_{l=1}^{n}\left[\left(L_{kl}(i_k,\theta) + i_k(t).\frac{\partial L_{kl}}{\partial i_k}\right)\frac{di_k}{dt} + i_k(t).\frac{\partial L_{kl}}{\partial \theta}.\omega\right] \quad (3)$$

where

$$\omega = \frac{d\theta}{dt} \quad (4)$$

is the angular speed of the SRM. Neglecting the mutual inductances, the instantaneous *k*-th phase voltage can be rewritten as follows:

$$V_k(t) = R_k i_k(t) + \left(L_k(i_k,\theta) + i_k(t).\frac{\partial L_k}{\partial i_k}\right)\frac{di_k}{dt} + i_k(t).\frac{\partial L_k}{\partial \theta}.\omega \quad (5)$$

where $L_k(i_k, \theta)$ denotes the *k*-th phase bulk inductance. The mechanical equation describing the motion of an SRM is given as:

$$J.\frac{d\omega}{dt} = T - T_L - f.\omega \quad (6)$$

where *J, f, T_L* and *T* are the total inertia, the friction coefficient, the load torque and the total output torque, respectively. The total output torque is calculated as:

$$T = \sum_{k=1}^{n} T_k(i_k,\theta) \quad (7)$$

where $T_k(i_k, \theta)$ denotes the *k*-th phase torque, which can be computed depending upon the derivative of the co-energy. The mathematical model of an SRM represented in (2), (4) and (6) can be applied to design the control strategies, which will be discussed below.

3. Fundamental Fuzzy Logic-Based Speed Control Architecture for the SRM Drive

The basic architecture of the conventional PI-based FL speed controller for an SRM drive system is described in Figure 2. In this control strategy, two inputs $(e_N[j], \Delta e_N[j])$ and one output $(\Delta u_N[j])$ are used for the FL inference system. Such two inputs are directly proportional to the error of the angular speed $e[j]$ and its change $\Delta e[j]$ through two gains K_1 and K_2, respectively. Meanwhile, the output is employed to generate the control signal $u[j]$, which is fed directly to the SRM drive model.

The architecture of an FLC includes three basic blocks: the knowledge base which contains rule base, data base and the inference mechanism, the fuzzification and the defuzzification interface [19]. Each block performs a particular functionality for the implementation of this FLC. In general, the first block (fuzzification) is used to convert the inputs into fuzzy sets. Subsequently, the second mechanism, that its operation is based on the rule base, will process the fuzzy sets which are obtained in the previous phase. Finally, the defuzzification is used to convert the results achieved above into the corresponding outputs of the FLC. It is the fact that all of the inputs and output of an FLC should be considered as crisp signals when they are processed.

For designing the FL reasoning system, two important issues need to be solved. The first problem is to determine the membership functions applied to such an FL model. Basically, three typical types of the membership functions can be used, including triangular, trapezoidal and Gaussian categories [19]. In the context of this work, the last type is chosen for all of two inputs and one output of the FL reasoning. In principle, each Gaussian membership function, $\mu_{Ai}(x)$, is mathematically formulated as follows:

$$\mu_{Ai}(x) = \exp\left(-\frac{(x-c_i)^2}{2\sigma_i^2}\right) \quad (8)$$

where c_i and σ_i denote respectively the center and width of the *i*-th fuzzy set of the membership function.

In this study, seven logic levels are used for each Gaussian membership function of two inputs and one output of the proposed PI-type FL controller.

The second important thing for designing the FL architecture is to build the rule base. For a conventional PI-type FLC, the basic 49-rule base is used as reported in [20]. It would be suitable to attain the high performances for a control drive system.

Basically, the principle of a PI-type FLC relies upon the crisp relationship between its inputs and output, which is similar to the classical PI regulator. The classical PI regulator is expressed as follows:

$$u(t) = K_p.e(t) + K_I.\int_0^t e(\tau)d\tau \qquad (9)$$

where K_P, K_I, $e(t)$ and $u(t)$ denote the proportional gain, the integral constant, the input error signal and the output of the regulator, respectively. Using the derivation, (9) can be rewritten as:

$$\frac{d}{dt}u(t) = K_p.\frac{d}{dt}e(t) + K_I.\mathrm{e}(t). \qquad (10)$$

Converting (10) into the discrete form, we yield:

$$\Delta u[j] = K_P.\Delta e[j] + K_I.e[j]. \qquad (11)$$

From Figure 2, the relationship between two inputs and one output of the FL inference can be written as:

$$\Delta u[j] = K_3.(\mu_1.K_1.e[j] + \mu_2.K_2.\Delta e[j]) \qquad (12)$$

where K_i (i = 1, 2, 3) and μ_k (k = 1, 2) are scaling factors and internal gains of the FL reasoning. Hence, from (12), one can be drawn below

$$\Delta u[j] = K_P^{FLC}.\Delta e[j] + K_I^{FLC}.e[j]. \qquad (13)$$

Two factors mentioned in (13), $K_P^{FLC} = \mu_2.K_2K_3$ and $K_I^{FLC} = \mu_1.K_1K_3$, can be considered as the proportional and integral gains compared with those of the classical PI regulator (see (9)). In order to determine such two factors, the PSO algorithm will be adopted in this work as presented in the following section.

4. Adaptive PSO-PI-type Fuzzy Logic-Based Speed Control Architecture

4.1. PSO Mechanism for Optimization problem

As presented in literature [22-24], PSO algorithm, considered as a well-known biological-inspired optimization technique, is described briefly below.

It is assumed that there are n random particles of a swarm relating to an n-dimensional variable space. Besides, m swarms can be chosen to enhance the ability of the optimization method. At the beginning, each individual is initialized with a stochastic position and velocity (typically belong to a uniform distribution with the corresponding lower and upper bounds). Normally, two vectors with parameters used in the i-th swarm at the beginning (t = 0) would be $\vec{P}_i^0 = \left(x_{i,1}^0, x_{i,2}^0, \ldots x_{i,n}^0\right)$ and $\vec{V}_i^0 = \left(v_{i,1}^0, v_{i,2}^0, \ldots v_{i,n}^0\right)$. Additionally, the lower and upper constraints of a swarm should be given by two vectors ($\vec{Lb}$ and $\vec{Ub}$). Also, to evaluate the convergence of each swarm when running the PSO mechanism, an objective function, f_{obj}, should be defined. This function will be calculated and compared to determine the local optimal parameters $\vec{P}_{i,best}$ at each time. The local optimal values obtained are then assessed to recognize the global optimal value $\vec{G}_{best}$. The determination of $\vec{P}_{i,best}$ and $\vec{G}_{best}$ must be conducted from the beginning (t = 0) to the final iteration (t = N). To continue the mechanism, each iteration should be updated. At time k (or the k-th iteration), both the velocity and position vectors of the i-th swarm can be updated by using the following two equations:

$$\vec{V}_i^{k+1} = \omega.\vec{V}_i^k + c_1r_1\left(\vec{P}_{i,best}^k - \vec{P}_i^k\right) + c_2r_2\left(\vec{G}_{best}^k - \vec{P}_i^k\right) \qquad (14)$$

$$\vec{P}_i^{k+1} = \vec{P}_i^k + \vec{V}_i^{k+1} \qquad (15)$$

where, c_1 and c_2 are two learning factors, r_1 and r_2 denote the random positive numbers belonging to the interval [0, 1]. Meanwhile, ω is an inertia weighted factor. Updating these two vectors, they should satisfy the constraint of the search problem. In addition, at each of iterations, both the local and global optimal values should also be updated. It is noted that, when implementing the PSO mechanism, the stop criteria should be checked any time. Normally, a stop criterion would be the maximum value of the iterations or an acceptable value of the objective function. If one of these criteria is met, the algorithm will be terminated.

4.2. Design an Adaptive PI-based Speed Controller Using the PSO Algorithm

In order to design an adaptive speed controller for the SRM drive using the FL technique, the PSO will be adopted. The proposed control scheme, modified from Figure 2, is illustrated in Figure 3.

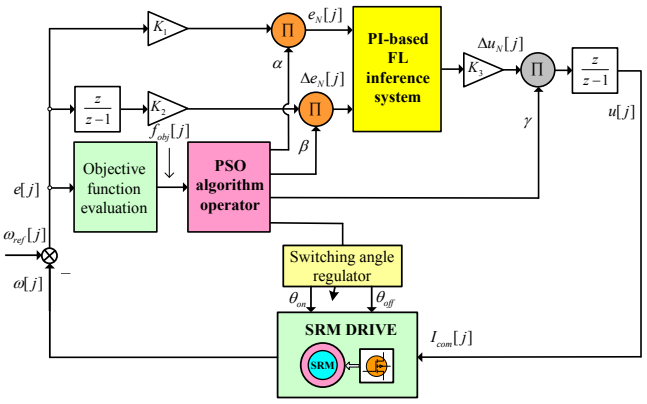

Figure 3: Improved speed controller architecture based on PI-type FL for SRM

For a PI-type FL controller, it is highly necessary to determine the optimal values of K_P^{FLC} and K_I^{FLC} since they can affect strongly the output signal, and hence impact on the control quality of the system. The PSO algorithm will be employed in this work to determine three scaling factors of the FL speed controller applied

to an SRM drive. This means that each group of coefficients K_i (i = 1, 2, 3) expressed in (12) will be modified by using three updating factors α, β, and γ, respectively (see Figure 3). The new factors are able to be obtained as follows:

$$K'_P = \mu_2.(\beta.K_2).(\gamma.K_3) \quad (16)$$

$$K'_I = \mu_1.(\alpha.K_1).(\gamma K_3). \quad (17)$$

As mentioned earlier, the objective function is highly important for performing the PSO mechanism. Here, it can be defined depending upon the crucial aims of an effective speed controller. Obviously, such a speed regulator must be able to attain the minimum rise time and settling time as well as no overshoot. Thus, an objective function can be utilized as:

$$f_{obj} = \int_0^t t.e(t)dt = \int_0^t t.\left(\omega_{ref} - \omega(t)\right)dt. \quad (18)$$

It is clear that f_{obj} needs to be minimized to meet an acceptable value, following the working mechanism of the PSO. The feasibility of the proposed adaptive PSO-FL-based control methodology will be validated through numerical simulation presented in Section 5.

4.3. Optimization of Switching Angles Applying the PSO Method

In this study, the PSO algorithm is applied to determine not only the scaling factors of the PI – type FLC but also the switching angles, namely, turn-ON angle θ_{ON} and turn-OFF angle θ_{OFF}. It is the fact that such two switching angles impact significantly on the electromagnetic torque generation of the SRMs [2-4]. The control performances of an SRM drive system will also be affected as a result, leading to the need of optimizing such two factors.

In the context of this study, θ_{ON} and θ_{OFF} can also be optimized by using the PSO method. To perform it, two arguments need to be added to the variable space of the PSO algorithm. Hence, there are totally five variables used in such PSO method, including three for gain updating factors (α, β and γ) and two for switching angles (θ_{ON} and θ_{OFF}). Using the trial and error method, the lower and upper bounds of the turn-ON angle and the turn-OFF angle applied in the case study of a three-phase SRM drive (6/4-type machine) can be determined respectively as follows:

$$30° \le \theta_{ON} \le 45° \quad (19)$$

$$70° \le \theta_{OFF} \le 87° \quad (20)$$

The optimization process based on the PSO algorithm will be carried out as mentioned earlier. Accordingly, the optimal control strategy proposed will be represented finally in Figure 3. The effectiveness and feasibility of the proposed control strategy will be discussed in the following section.

5. Numerical Simulation

In this section, numerical simulation processes using MATLAB/Simulink package will be implemented to verify the superiority and feasibility of the proposed control architecture. The simulation diagram built in Simulink environment is dependent upon Figure 3 for a typical three-phase SRM (6/4-type machine). In this work, to validate the outstanding performances of the proposed FL-based speed control strategy, a conventional speed regulator using PI will also be utilized. On the other hand, to simplify the control execution, the PI-type current controllers are employed for the SRM drive. The PSO algorithm, which is executed by an *m*-file written in MATLAB/Script environment, will be applied to design the adaptive control methodology as mentioned earlier. Based on the implementation of the PSO method, two simulation cases are considered as:

(i) Case 1: The PSO algorithm is only applied to optimize three updating factors in order to design an adaptive PSO-PI-type FL speed controller. In this case, two switching angles are determined by using the trial and error method. In addition, a load torque condition (T_L = 100 *N.m*) is taken to the SRM drive at 0.6*s* to evaluate the dynamic behavior of the control system using different controllers.

(ii) Case 2: The PSO algorithm is used to determine not only three updating factors but also two switching angles. Hence, in this case, there are totally five variables need to be optimized in order to design the adaptive control methodology for the SRM drive. A complex-practical load torque, which will be mentioned below, is applied to this case to obtain an effective comparison between two control strategies, i.e., the conventional PI speed regulator and the adaptive PSO-PI-type FL speed controller.

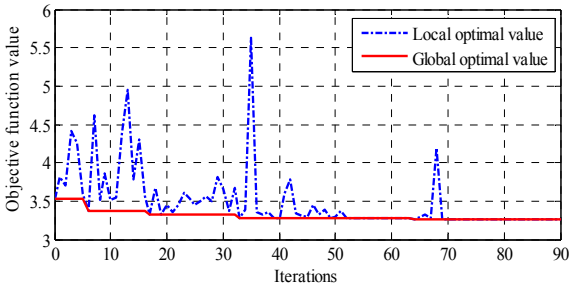

Figure 4: General convergence of the PSO mechanism in the first simulation case

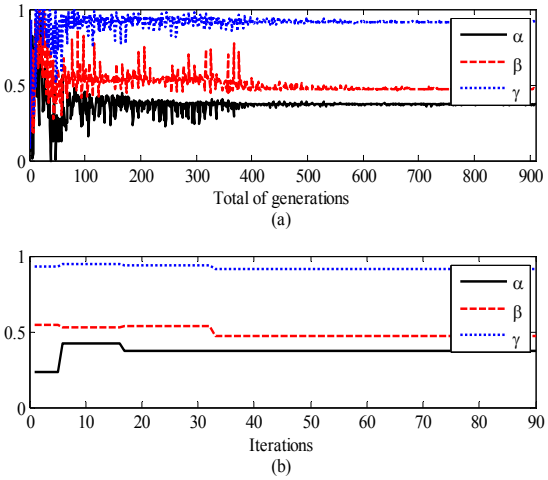

Figure 5: Convergence of three updating factors in the first simulation case

Simulation parameters are given in the Appendices of the present paper. The simulation results for the first case are described in Figures 4-6. Meanwhile, Figures 7-12 show the results for the second simulation case.

In the first simulation case, as shown in Figure 4, the convergence representing the objective function value of the PSO method (with N = 90) can be obtained. On the other hand, all of three updating factors (α, β and γ), illustrated in Figure 5, are also converged towards the constant values after a few dozen iterations of the PSO implementation. Applying such three factors, together with two switching angles obtained by using the trial and error method (i.e., $\theta_{ON} = 44°$ and $\theta_{OFF} = 79°$), the dynamic responses of the angular speed for two controllers, PI and PSO-PI-type FL, can be achieved as plotted in Figure 6. It is found clearly that the proposed FL-based controller obtains the better control performances in comparison with the conventional PI regulator. The angular speed resulting from the proposed control methodology is able to reach the reference value ($\omega_{ref} = 1000rpm$) much faster. Furthermore, even when a load torque occurs ($T_L = 100\ N.m$ at 0.6s), the dynamic response of the PSO-PI-type FL controller is still efficient enough to recover the constant value of the speed as rapidly as possible. In contrast, at that moment, the angular speed resulting from the conventional PI regulator is fallen and may not be able to recover the constant reference value within a small period (see Figure 6). Two speed deviations before and after the load torque appearance (i.e., $\Delta\omega_1$ and $\Delta\omega_2$) reveal the outperformance of the proposed control architecture for the SRM drive.

In the second simulation case, with five variables need to be optimized, the convergence of the PSO mechanism can be attained as described in Figures 7-9. Here, a complicated-practical load torque, shown in Figure 10(a), is embedded in the drive system. With the enough number of iterations (N = 100), the value of the convergent objective function is much smaller than that of the first case (see Figures 4 and 7). This reveals that the controller applying the PSO algorithm in this case can obtain the better control qualification. Figure 10(b) shows the transient speed resulting from two controllers considered in this paper. Similar to the first case, when treating a reference speed (ω_{ref} = 1200rpm), the proposed FL control architecture can achieve the steady state much more quickly than the conventional PI-based scheme. In addition, there is no reduction of the speed due to the load occurrence when applying the PSO-PI-type FL speed controller. This is obviously impossible to be obtained when using the PI speed regulator. Here, the maximum speed reduction resulting from such a PI regulator can be calculated as follows:

$$\Delta\omega_{\max} = \max_{t_0 \le t \le t_{\max}} \left(\omega_{ref} - \omega(t)\right) \qquad (21)$$

where t_0 is the time at which the load torque is embedded and t_{max} is the maximum simulation time. Using (21), the maximum speed reduction in this case is greater than 110 rpm, representing approximately 10% of the reference value. This leads to the drawback of the conventional PI regulator when applied to control the speed of an SRM drive system. On the other hand, this further demonstrates the superiority of the proposed PSO-based FL controller when maintaining the angular speed of the machine. Figures 11 and 12 illustrate the dynamic responses of phase currents and total torque resulting from two speed controllers. Obviously, the adaptive FL speed controller can achieve the larger starting and running torques in comparison with those of the PI regulator. It is highly meaningful to choose a type of drive motors to design an effective traction control system (TCS) in reality, such as the TCS in an electric vehicle.

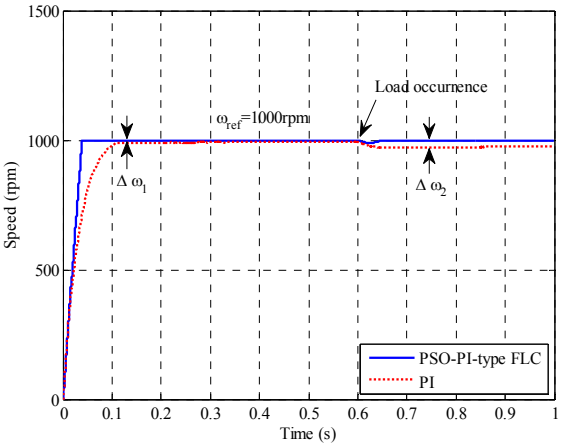

Figure 6: Speed response for the first simulation case

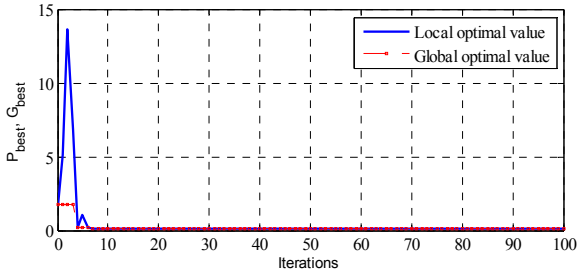

Figure 7: PSO general convergence in the second case

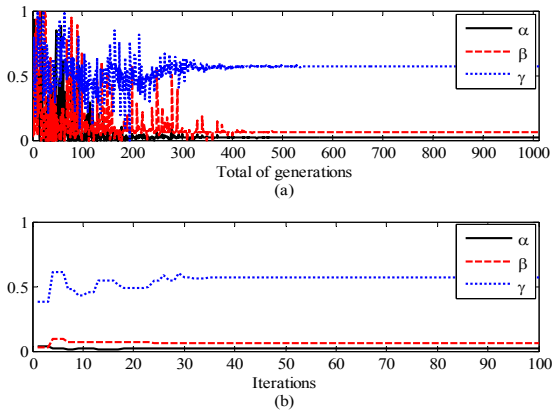

Figure 8: Convergence of three updating factors in the second case

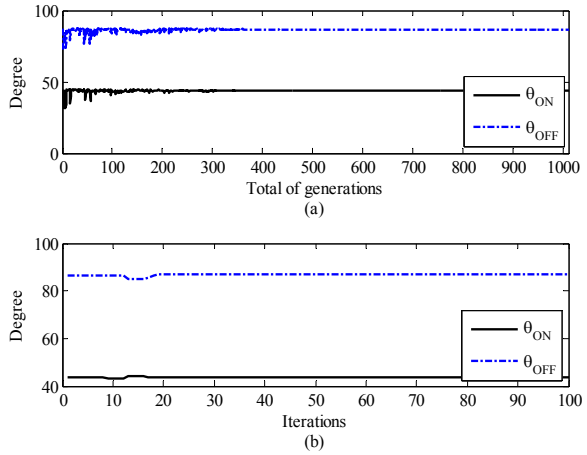

Figure 9: Convergence of two switching angles in the second case

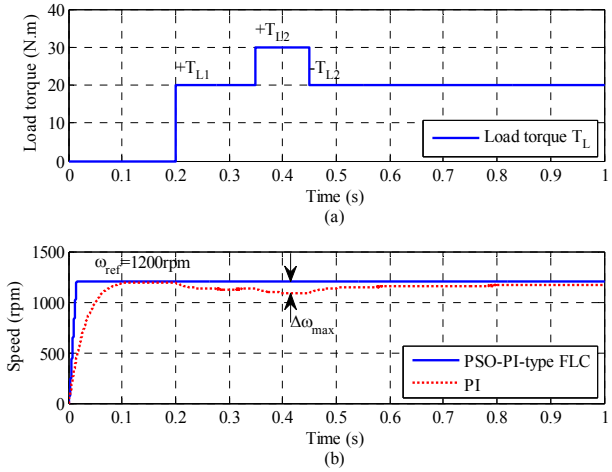

Figure 10: Load and speed response in the second case
(a) Load torque
(b) Dynamic response of the speed

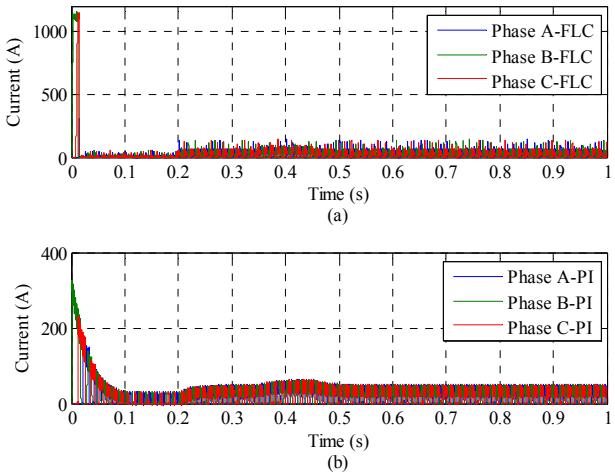

Figure 11: Dynamic response of three phase currents in the second case
(a) For PSO-PI-type FLC
(b) For the conventional PI controller

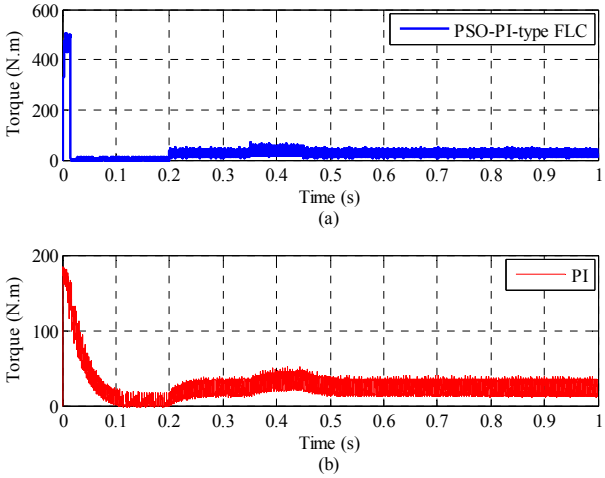

Figure 12: Dynamic response of moment in the second case
(a) For PSO-PI-type FLC
(b) For the conventional PI controller

6. Conclusions and Discussions

The design of an adaptive PSO-based PI-type FL speed control strategy for the SRM drive systems has been investigated in this paper. In principle, the PSO algorithm is applied to tune three scaling factors of the PI-type FL reasoning system as well as two switching angles of an SRM, which can affect strongly the control performances of the drive system. Numerical simulation results for a typical three phase SRM drive applying two types of the speed controllers (i.e., conventional PI and adaptive PSO-PI-based FL regulator) with various cases of the load torques have demonstrated the feasibility and effectiveness of the proposed control methodology. The dynamic responses of the angular speed resulting from the adaptive FL controller are much better than those of the conventional PI regulator. Along with the large starting and running torque obtained, the SRM drive system applying the proposed control architecture is able to become a perfect candidate when designing an effective traction control system.

For future work, different types of the switched reluctance machines, such as 8/6, 10/8 or 12/8, should be considered to extend the application of the proposed control methodology. With the increasing development of the artificial neural network (ANN) technique, a category of the hybrid controller applying the FL and ANN architecture as well as the biological-inspired optimization methods (e.g., the PSO and Genetic Algorithm) should also be investigated to further enhance the control performances of an SRM drive system. Therefore, the promising results obtained from this study will motivate the future work in order to seek an effective and modern drive solution applying the novel family of the machines, replacing the conventional engines, such as the induction motor (IM) or synchronous motor (SM).

Appendices

Parameters a 6/4 SRM model

$R_k = 0.05\Omega, J = 0.05kg.m^2, f = 0.02N.m.s$

$L_k^{\min} = 0.67mH, L_k^{\max} = 23.6mH, i_k^{\max} = 500A$

PSO parameters

The first simulation case:

$n = 3, m = 10, N = 90, \overrightarrow{Lb} = [0,0,0], \overrightarrow{Ub} = [1,1,1]$

The second simulation case:

$n = 5, m = 10, N = 100$

$\overrightarrow{Lb} = [0,0,0,30,70]; \overrightarrow{Ub} = [1,1,1,45,87]$

Acknowledgment

This work was supported by the National Natural Science Foundation of China (Grants No: 6117075, 60835004 and 61104088), the National High Technology Research and Development Program of China (863 Program) (2012AA111004, 2012AA112312).

References

1. Balaji, M.; Kamaraj, V.: *Evolutionary computation based multi-objective pole shape optimization of switched reluctance machine*. Electr. Power Energy Syst. 43(1), 63-69, 2012.
2. Peter, B.: *3-Phase Switched Reluctance Motor Control with Encoder Using 56F805*. Motorola Czech System Laboratories, Czech Republic, 2003.
3. Krishnan, R.: Switched Reluctance Motor Driver: Modeling, Simulation, Analysis, Design, and Applications. CRC Press, New York, 2001.
4. Ahmad, M.: High Performance AC Drives Modeling Analysis and Control. Springer, London, UK, 2010.
5. Zhengyu, L.; Reay, D.S.; Williams, B.W.; Xiangning H.: *Torque Ripple Reduction in Switched Reluctance Motor Drives Using B-Spline Neural Networks*. IEEE Trans. Ind. Appl. 42(6), 1445-1453, 2006.
6. Xue, X.D.; Cheng, K.W.E.; Lin, J.K.; Zhang, Z.; Luk, K.F.; Cheung, N.C.: *Optimal control method of motoring operation for SRM drives in electric vehicles*. IEEE Trans. Veh. Technol. 59, 1191-1204, 2010.
7. Santos, D.F.L.M.; Anthonis, J.; Naclerio, F.; Gyselinck, J.J.C.; Auweraer, V.D.H.; Goes, L.C.S: *Multiphysics NVH modeling: simulation of a switched reluctance motor for an electric vehicle*. IEEE Trans. Ind. Electron. 61, 469-476, 2014.
8. Kiyota, K.; Kakishima, T.; Chiba, A.: *Comparison of test result and design stage prediction of switched reluctance motor competitive with 60-kW rare-earth PM motor*. IEEE Trans. Ind. Electron. 61, 5712-5721, 2014.
9. Bilgin, B.; Emadi, A.; Krishnamurthy, M.: *Comprehensive evaluation of the dynamic performance of a 6/10 SRM for traction application in PHEVs*. IEEE Trans. Ind. Electron. 60: 2564-2575, 2013.
10. Sunan, E.; Kucuk, F.; Goto, H.; Guo, H.J.; Ichinokura, O.: *Three-phase full-bridge converter controlled permanent magnet reluctance generator for small-scale wind energy conversion systems*. IEEE Trans. Energy Conver. 29(3): 585-593, 2014.
11. Wang, H.; Liu, J.; Bao, J.; Xue, B.: *A novel bearingless switched reluctance motor with a biased permanent magnet*. IEEE Trans. Ind. Electron. 61(12): 6947-6955, 2014.
12. Mendez, S.; Martinez, A.; Millan, W.; Montano, C.E.; Cebolla, F.P.: *Design, characterization, and validation of a 1-kW AC self-excited switched reluctance generator*. IEEE Trans. Ind. Electron. 61(2): 846-855, 2014.
13. Andrada, P.; Blanque, B.; Martinez, E.; Torrent, M.: *A novel type of hybrid reluctance motor drive*. IEEE Trans. Ind. Electron. 61(8), 4337-4345, 2014.
14. Lee, D.H.; Lee, Z.G.; Liang, J.; Ahn, J.W.: *Single-phase SRM drive with torque Ripple reduction and power factor correction*. IEEE Trans. Ind. Appl. 43(6), 1578-1587, 2007.
15. Madhavan, R.; Fernandes, B.G.: *Performance improvement in the axial flux-segmented rotor-switched reluctance motor*. IEEE Trans. Energy Conver. 29(3), 641-651, 2014.
16. Cai, J.; Deng, Z.; Hu, R.: *Position signal faults diagnosis and control for switched reluctance motor*. IEEE Trans. Magn. 50(9), 1-11, 2014.
17. Dursun, M.; Koc, F.: *Linear switched reluctance motor control with PIC18F452 microcontroller*. Turk. J. Elec. Eng. & Comp. Sci. 21, 1107-1119, 2013.
18. Jihong, L.: *On methods for improving performance of PI-type fuzzy logic controllers*. IEEE Trans. Fuzzy Syst. 1(4), 298-301, 1993.
19. Bimal, K.B.: Modern power electronics and AC drives. Prentice Hall PTR, Upper Saddle River, NJ, USA, 2002.
20. Mudi, R.K.; Pal, N.R.: *A robust self-tuning scheme for PI- and PD-type fuzzy controllers*. IEEE Trans. Fuzzy Syst. 7(1), 2-16, 1999.
21. Mir, S.; Islam, M.S.; Sebastian, T.; Husain, I.: *Fault-tolerant switched reluctance motor drive using adaptive fuzzy logic controller*. IEEE Trans. Power Electr. 19(2), 289-295, 2004.
22. Yamille, D.V.; Ganesh, K.V.; Salman, M. ; Jean-Carlos, H., Ronald, G.H, : *Particle swarm optimization : basic concepts, variants and applications in power systems*. IEEE Trans. Evol. Comput. 12(2), 171-195, 2008.
23. Bevrani, H.; Habibi, F.; Babahajyani, P.; Watanabe, M.; Mitani, Y.: *Intelligent frequency control in an AC microgrid: online PSO-based fuzzy tuning approach*. IEEE Trans. Smart Grid. 3(4), 1935-1944, 2012.
24. Noureddine, B.; Djamel, B.; Boudjema, F.: *Tuning fuzzy fractional order PID sliding-mode controller using PSO algorithm for nonlinear systems*. In: Systems and Control (ICSC) International Conference, Algiers, Algeria, pp. 797-803, 2013.